Battery-Free Cellphone

VAMSI TALLA, BRYCE KELLOGG, SHYAMNATH GOLLAKOTA AND JOSHUA R. SMITH,
Paul G. Allen School of Computer Science and Engineering and Department of Electrical Engineering, University of Washington

We present the first battery-free cellphone design that consumes only a few micro-watts of power. Our design can sense speech, actuate the earphones, and switch between uplink and downlink communications, all in real time. Our system optimizes transmission and reception of speech while simultaneously harvesting power which enables the battery-free cellphone to operate continuously. The battery-free device prototype is built using commercial-off-the-shelf components on a printed circuit board. It can operate on power that is harvested from RF signals transmitted by a basestation 31 feet (9.4 m) away. Further, using power harvested from ambient light with tiny photodiodes, we show that our device can communicate with a basestation that is 50 feet (15.2 m) away. Finally, we perform the first Skype call using a battery-free phone over a cellular network, via our custom bridged basestation. This we believe is a major leap in the capability of battery-free devices and a step towards a fully functional battery-free cellphone.

CCS Concepts: •**Computer systems organization** →**Embedded and cyber-physical systems;** •**Human-centered computing** →*Ubiquitous and mobile computing;*

Additional Key Words and Phrases: Battery-free phone; RF-power & photodiode harvesting; Backscatter communication.

ACM Reference format:
Vamsi Talla, Bryce Kellogg, Shyamnath Gollakota and Joshua R. Smith. 2017. Battery-Free Cellphone. *PACM Interact. Mob. Wearable Ubiquitous Technol.* 1, 2, Article 25 (June 2017), 20 pages.
DOI: http://doi.org/10.1145/3090090

1 INTRODUCTION

This paper asks the following question: Can we design a battery-free cell phone that operates while consuming only a few micro-watts of power? Given that batteries add weight, bulk, cost, require recharging and replacement, a positive answer would enable phones that have two-way communication capabilities without the need for batteries. Further, a microwatt-power phone can use cheap and lightweight harvesting sources including radio signals and photodiodes instead of bulky and expensive solar cells. Finally, such a design would represent a fundamental leap in the capability of battery-free devices.

The key challenge in achieving this is that a cellphone is required to perform multiple basic operations: sensing speech at the device, transmitting it to the base station, receiving speech information from the base station and finally actuating the speaker/earphones. Designing a battery-free cell phone system requires us to perform all these functions, in real time, using only a few micro-watts of power.

To appreciate this challenge, it is instructive to look at existing low-power battery-free sensor prototypes. RF-powered sensors such as accelerometers [35], humidity [34] and temperature sensors [35] are heavily duty-cycled to send sensor data once every few seconds or minutes. RF-powered cameras [27, 37] require extensive

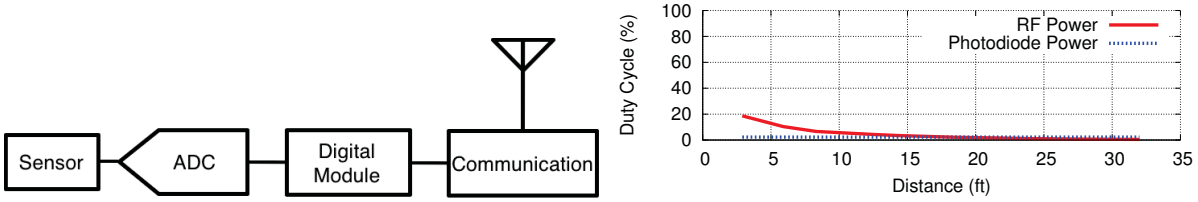

(a) System architecture for existing digital approach.

(b) Duty cycle while transmitting speech on RF power using existing digital approach.

Fig. 1. **Digital approach for sensing.** (a) shows the system architecture for existing wireless sensors and (b) shows the corresponding duty cycle for a wireless digital microphone. We use ADMP801 microphone which consumes 15.3 μW as our sensor [1]. We digitize the output of the microphone with 8-bit internal analog to digital converter (ADC) of MSP430FR5969 micro-controller at 8 kHz sampling rate. We transmit data using digital backscatter back to a basestation. The system consumes an average power of 1 mW while its transmitting speech at 8 kHz. We conduct similar experiment when device is powered by photodiodes (see §4.1.2 for details) harvesting ambient light of 500 Lux.

duty-cycling of tens of minutes to harvest enough energy to capture, process and communicate a single frame. In contrast, cellphones have to sense speech, actuate the speaker/earphones, and switch between uplink and downlink communications, all in real time. This imposes significant constraints on the system.

We present the first battery-free cellphone design that consumes only a few micro-watts of power. To achieve this goal, we perform a significant re-design of the battery-free system architecture. In particular, Fig. 1(a) shows the architecture of existing battery-free systems: the sensing and the communication modules are interfaced through a digital computing module (e.g., micro-controller/Field Programmable Gate Array). An ADC digitizes the sensor input to be processed by the micro-controller, which is then connected to a communication module. The problem is that this architecture is not compatible with real-time operations for the following reasons:

- While communication can be make power efficient using backscatter, digital computational modules such as micro-controllers and Field Programmable Gate Arrays (FPGAs) are the bottleneck in the above architecture. Specifically, these modules consume orders of magnitude more power than our target power consumption.
- The above architecture requires power-hungry ADCs and digital to analog converter (DACs) to interface between the sensors and the computing modules [39]. Further, since we lose information about changes smaller than the discrete levels in an ADC, we need an automatic gain control module to adapt to the variations in the wireless channel. All these functions consume power, significantly limiting our ability to operate in real time.

To illustrate the limitations of the above battery-free design, we measure the performance of a wireless digital microphone system using both RF and photodiode power harvesting. Fig. 1 plots the duty cycle as a function of distance from the basestation that receives the microphone data for both a RF-powered microphone and a photodiode powered microphone. The RF powered microphone can operate at 20% duty cycle at 3 feet and a 5% duty cycle at a distance of 10 feet from the basestation. The photodiode powered version has a constant duty cycle of 2.5% for an ambient light setting of 500 Lux. The key challenge here is that ADCs and digital computation consume milli-watts of power whereas only micro-watts of harvested power is available. This forces existing battery-free devices to extensively duty cycle their operations.

To overcome these challenges, we present the architecture shown in Fig. 2 which *bypasses* the computational module between the sensors and communication. In particular, on the uplink, instead of using an ADC to digitize the sensor signals and then again creating the RF signals using backscatter, we eliminate this power-consuming conversion process to create a purely analog system that feds the analog sensor data directly to the backscatter module. We design an impedance matching network to interface the analog sensor, i.e., electret microphone to the antenna which maximizes the backscattered analog speech signal while simultaneously harvesting power to

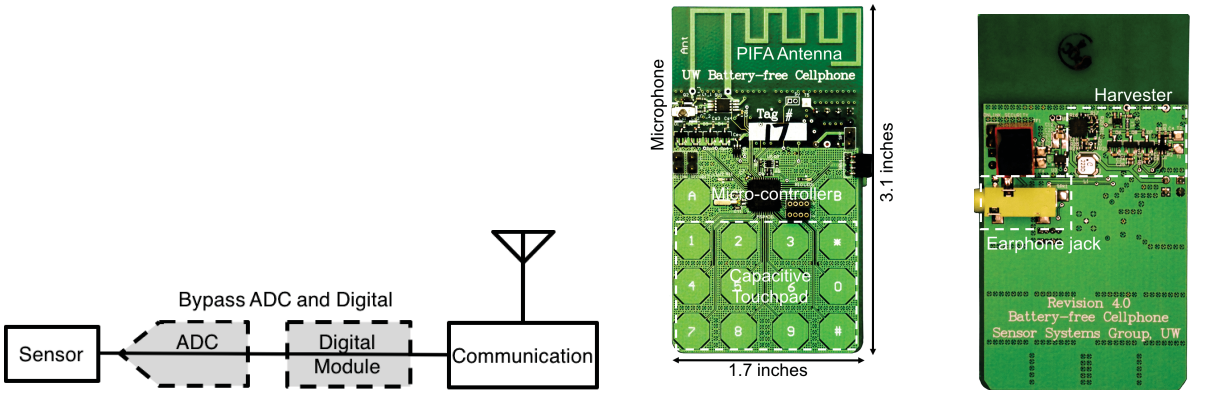

(a) Proposed architecture (b) Front of the battery-free phone (c) Back of the battery-free phone

Fig. 2. **Battery-free phone prototype.** Our architecture which bypasses the computational module between sensors and communication. We also show the front and back of the PCB prototypes of the battery-free phone.

enable continuous battery-free operation. Similarly, on the downlink, instead of sending digital data to the device from the basestation, which is then fed into earphones using a DAC, the basestation sends analog speech data encoded in the RF transmissions that directly actuate the headphones. We optimize the envelope of the speech encoded RF transmissions from the basestation and design an optimal downlink impedance matching network to simultaneously receive speech and harvest power from RF transmissions and enable continuous battery-free phone operation.

We implement the battery-phone cellphone using commercial off-the shelf (COTS) components on a printed circuit board (PCB). We use a 2 dBi gain printed inverted F antenna (PIFA) in our design as shown in Fig. 2. The PIFA antenna design is a good tradeoff between size, non-directionality and efficient operation with a relatively large ground plane. Our prototype comes complete with capacitive touch buttons and LEDs to interact with the user. Our device uses RF as well as photodiode harvesters to convert incident RF and ambient light respectively into DC output. The RF powered device has the advantage of reusing the communication antenna for power thereby reducing the cost and size of the device and can operate up to 31 feet from the basestation. Additionally, the RF powered device can operate independent of weather and lighting conditions. The photodiode powered cellphone uses a tiny photodiode (1.1 cm^2) to convert 500 lux ambient light into DC power and can operate up to 50 feet from the basestation.

In summary, this paper makes the following key technical contributions:

- We integrate an analog backscatter microphone and an AM receiver into a single platform to transmit and receive speech on a battery-free system, creating the first battery-free cellphone that consumes only a few micro-watts. Our battery-free system can continuously operate on power harvested from RF signals transmitted by a basestation as well as ambient light using tiny photodiodes.
- We jointly optimize the energy harvesting, analog speech transmission and analog speech reception for different harvesting approaches. Specifically, we design optimal impedance matching networks for backscatter microphones to continuously transmit speech and AM receivers to continuously receive speech. We design matching networks for both RF and photodiode powered phones.
- We perform the first Skype call using a battery-free cellphone. Specifically, the battery-free cellphone communicates speech and state information with the basestation, while the latter interacts with cellular networks using a Skype plugin and bridges the connection between our cellphone and cellular networks.

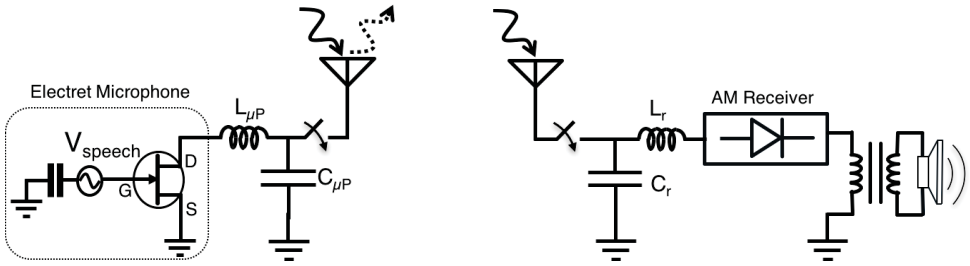

(a) System architecture for transmitting speech at the battery-free phone

(b) System architecture for receiving speech from the battery-free phone

Fig. 3. **Architecture for transmitting and receiving speech.** We show the architecture of the system used to transmit and receive speech at the battery-free phone using analog approaches.

2 OVERVIEW

A cellphone is required to perform three basic operations: communicate and co-ordinate with a base station, sense and transmit speech and receive speech and actuate the speakers. The battery-free device performs all these operations by leveraging a dedicated basestation. At a high level, we delegate all the power-hungry components and operations such as coordinating and communication with cellular networks to the basestation.

At the physical layer, the battery-free cellphone communicates exclusively with the basestation which is responsible for bridging the connection between the phone and cellular network. The phone uses analog backscatter to directly transmit speech from a passive microphone and amplitude modulation to receive analog speech from the basestation. The phone uses existing digital backscatter techniques to communicate state information and co-ordinate with the basestation. Backscatter transmitters are 3–4 orders of magnitude lower power compared to radios and minimize the power consumption of the phone [24]. Basestation transmits digital data by encoding information in the presence and absence of an RF carrier. The phone uses an envelope detector based receiver to decode digital bits while consuming a few micro-watts of power [26]. The basestation uses Skype API to establish and manage connection with cellular networks. It implements a custom state machine to co-ordinate the connection between the cellular network and battery-free cellphone.

3 BATTERY-FREE SPEECH TRANSMISSION AND RECEPTION

Existing ADC and DAC based approaches to transmitting and receiving speech consume too much power to be applicable for real-time battery-free applications. To address these shortcomings, we present analog techniques for speech transmission and reception that consume only a few microwatts of power.

3.1 Transmitting Speech from the battery-free phone

Our design takes inspiration from the Great Seal Bug [3] and uses analog backscatter. In analog backscatter, we directly backscatter speech from a passive microphone to the basestation. To understand this approach, let us look at the high-level architecture of our system shown in 3(a). It consists of an electret microphone (EK-23024-00 [4]) directly connected to the antenna via an RF switch. The RF switch is used to connect and disconnect the microphone from the antenna to configure the phone in speech transmit and other operating modes respectively. The control and operation of the RF switch is described in §4.

Electret microphone is a passive element which does not require any power. The sensing element in the microphone is a diaphragm that is separated by an air gap from a fixed metal back plate. The diaphragm and the metal plate form a capacitor. The diaphragm is made up of electret material that has a quasi-permanent electrostatic charge. When the sound waves move the diaphragm, the distance between the two plates of the

capacitor change, resulting in a change in capacitance. Since, the charge stored on the electret diaphragm is fixed, a small voltage V_{speech} is generated and the generated voltage is directly proportional to the volume of the speech at the diaphragm.

Internally, the capacitor is connected to the gate of a JFET. Traditionally, a JFET is configured as a common source voltage amplifier and is used to amplify the small voltage change. However, in our analog backscatter system, we leverage the fact that a JFET with $V_{GS} = 0$ bias point operates in the triode region and can be used as a trans impedance, i.e., voltage to impedance amplifier. So, the voltage from the capacitor V_{speech} changes the impedance between the drain and source terminals (R_{DS}) of the JFET. The JFET impedance in terms of V_{speech} can be mathematically written as, $R_{DS} = \frac{R_{DS_0}}{\left(1-\frac{V_{speech}}{V_p}\right)}$. Here V_p is the pinch-off voltage and R_{DS_0} is the impedance of the JFET for zero voltage at the gate terminal. To maximize the signal backscattered by the microphone, we tune the impedance of the JFET to match the impedance of the antenna using an L-C matching network. For typical quality factor (≥ 4) of the matching network, we can represent the impedance of the microphone seen by the antenna as,

$$R_{\mu P} = \frac{\omega^2 L_T^2}{R_{DS}} = R_0 \left(1 - \frac{V_{speech}}{V_p}\right) \tag{1}$$

Here R_0 is the impedance at the antenna terminal for no speech. The basestation is configured to transmit a single tone signal. Now, from backscatter theory [18], we know that the signal backscattered by the microphone can be written in terms of the reflection coefficient $\Gamma = \frac{R_a - R_{\mu P}}{R_a + R_{\mu P}}$ as,

$$S_{backscattered} \propto 1 + \Gamma = \frac{2R_a}{R_a + R_{\mu P}} = \frac{2R_a}{R_a + R_0\left(1 - \frac{V_{speech}}{V_p}\right)} \approx \frac{2R_a}{R_a + R_0}\left[1 + \frac{V_{speech}}{V_p}\left(\frac{R_0}{R_a + R_0}\right)\right] \tag{2}$$

For typical values of V_{speech} (tens of mV), we use binomial approximation to represent the backscattered signal as a linear function of the speech. This backscattered signal undergoes path loss and is received by the basestation. The first term in the above equation is at DC and the second term proportional to the transmitted speech is the desired signal. The desired backscattered signal is proportional to the voltage at the gate of the FET which is in turn directly proportional to the volume of the speech at the diaphragm of the microphone, i.e., louder the speech, stronger the backscattered signal. The basestation recovers the speech information from the backscattered RF signal by first down converting the RF signal to baseband followed by a 300 Hz to 3.4 kHz bandpass filter to eliminate the out of band noise. To maximize the backscattered speech signal, we set $R_0 = R_a$, i.e., we tune the impedance of the microphone when there is no input speech, to match the antenna impedance.

Using the above analog backscatter approach, we eliminate the need for continuously operating an on-board ADC and digital computation and instead delegate these power-hungry components to the basestation. In §4 we show that the computation block (MSP430 micro-controller) is only required to control an RF switch for connecting and disconnecting the microphone from the antenna and this switch consumes 0.22 μW of additional power. We note that in an analog backscatter system, the wireless signal first undergoes a path loss in the forward direction from the basestation to the battery-free phone and then back from the phone to the basestation. Thus, the backscattered signal attenuates as $\frac{1}{d^4}$ and the quality of the analog backscattered speech degrades as the distance between the basestation and the phone, d, increases.

3.2 Receiving Speech at the battery-free phone

Like speech transmission, conventional digital approaches for receiving speech are also too power expensive to be used in battery-free systems. A digital downlink communication link, followed by a DAC and an earphone driver add significant computational and power overhead making it impossible for battery-free systems to operate

continuously. Instead we take inspiration from crystal radios [40] and use amplitude modulated signal to transmit speech to a battery-free phone.

The architecture of our approach is shown in 3(b). The speech signal $s(t)$ varies between +1 and -1. The basestation encodes analog speech in the amplitude of the RF signal RF_{AM}. The amplitude modulated RF signal can be written as $RF_{AM} = \left\{1 + \frac{m}{2}(s(t) - 1)\right\} Acos(2\pi f_c t)$ where m is the modulation index, f_c is the carrier frequency and A is the maximum amplitude of the RF signal. We introduce a DC bias and normalize the speech signal by a factor of 2 to avoid distortion by ensuring that the amplitude of the RF carrier varies between 0 and A (since $0 \leq 1 + \frac{m}{2}(s(t) - 1) \leq 1$). The transmitted AM signal has two components: $\frac{m}{2} s(t) Acos(2\pi f_c t)$ and $\left(1 - \frac{m}{2}\right) Acos(2\pi f_c t)$. The first component is the time varying envelope of the signal and corresponds to the speech transmitted to the phone. Assuming that speech is a sinusoidal signal, the average power of the RF signal corresponding to the transmitted speech is $\frac{A^2 m^2}{4} \frac{1}{4}$ where $\frac{1}{4}$ is the power of multiplication of two independent sinusoids. The second component of the AM signal is available for RF harvesting and the harvestable power is given by $A^2 \left(1 - \frac{m}{2}\right)^2 \frac{1}{2}$. By varying the modulation index m we can tradeoff between the available power for RF harvesting and the power of the transmitted speech. In §5.1.2 and §5.3, we evaluate this tradeoff.

On the phone, as before, we use an RF switch to connect and disconnect the AM receiver from the antenna to configure the phone in speech receiving and other operating modes respectively. We use a passive 4-stage diode based envelope detector as the amplitude modulation (AM) receiver. The AM receiver filters out the carrier and tracks the envelope of the carrier to recover the transmitted speech. An audio transformer is used to interface the AM receiver directly to earphones without the need for any driver. The audio transformer is an impedance matching network that ensures that the low impedance earphones (18 Ω) do not load the output of the envelope detector. We use Moshi's Mythro earphones with high efficiency Neodymium drivers to maximize the volume of the output speech [5]. To maximize the power of the speech signal received by the phone, we use an L-C matching network to match the impedance of the AM receiver to the impedance of the antenna. This minimizes reflections at the antenna and maximizes the power received by the envelope detector that in turn optimizes the quality and volume of speech at the earphones.

As before, by using a purely analog approach, we eliminate the need for continuous operation of ADC and digital computation on the phone and delegate these power-hungry components to the basestation. Instead the phone uses passive zero power elements like an envelope detector, to recover the speech and actuates the earphones by using the energy of the incoming RF signal. In §4 we show that a computation block (MSP430 micro-controller) is required to control an RF switch for connecting and disconnecting the AM receiver from the antenna. The switch consumes only 0.22 μW of additional power. Since wireless signals attenuates as $\frac{1}{d^2}$ where d is the distance between the battery-free phone and the basestation the quality and volume of the received speech degrades as the distance between the basestation and the battery-free phone increases. We evaluate the quality of the received speech in §5.3.

4 DESIGN AND IMPLEMENTATION OF THE BATTERY-FREE PHONE

Fig. 4 shows the architecture of the battery-free phone. The RF or the photodiode harvester converts incident RF or ambient light respectively into DC output and powers the cell phone. Phone uses analog backscatter to directly transmit analog speech from a passive microphone and amplitude modulation to receive analog speech from the basestation. It also uses digital backscatter to occasionally communicate state information with the basestation. An MSP430 micro-controller (MSP430FR5969 [6]) implements a digital state machine to control different modules of the phone and co-ordinate with the basestation. Finally, the phone uses capacitive touch buttons and LEDs to interact with the user.

Table 1 summarizes the power consumption of the different components of the battery-free phone. The power harvester which includes power management consumes 2.15 μW of DC power. The RF switch which connects and

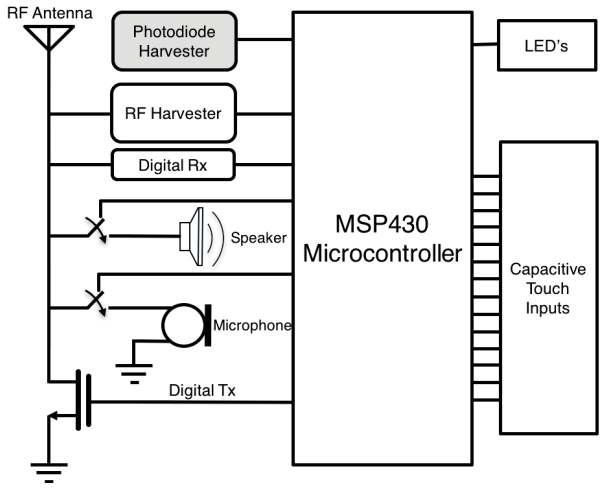

Fig. 4. **Architecture of the Battery-free phone**: The phone uses harvester to convert RF or ambient light into DC power. It uses analog backscatter to directly transmit analog speech from a passive microphone and amplitude modulation to receive analog speech from the basestation. The phone has an MSP430 micro-controller which implements a digital state machine and controls different modules of the phone. It also has capacitive touch buttons and LEDs to interact with the user and uses digital backscatter to occasionally communicate state information with the basestation.

Table 1. **Summary of the power consumption of battery-free phone**

Component	Power Consumption
Harvester & Power Management	2.15 μW
MSP430 micro-controller (LPM3)	0.86 μW
RF switch	0.22 μW
Biasing & Misc.	0.25 μW
Total	3.48 μW

disconnects the microphone and AM receiver from the antenna to switch between different modes consumes 0.22 μW. Finally, the MSP430 micro-controller which implements control and state machine operates in low power mode (LPM3) and has a quiescent power consumption of 0.86 μW. Thus, by using a combination of analog and digital approaches we operate the battery-free phone on a power budget of a few microwatts (3.48μW).

In the following section, we describe the design of different components of the battery-free cell phone. We start with our implementation of the RF and photodiode harvesters. Next, we describe techniques to optimize speech transmission and reception on an RF and photodiode powered cellphone. Finally, we describe how the user interacts with the phone as well as the digital state machine which controls different modules of the phone and interacts with the basestation.

4.1 Energy harvesting

The battery-free phone can harvest energy from either the RF signal transmitted by the basestation or from ambient light. In this section, we present the harvester design for both approaches. The RF energy harvester consists of a rectifier that converts the incident RF signal into low voltage DC power [37]. This power is fed to a DC–DC boost converter which increases the voltage to 1.8–2.4 V to match the requirements of the micro-controller and sensors. To harvest from ambient light, we use a photodiode and since the output is already a low voltage DC, we boost this voltage using a DC–DC boost converter to increase the voltage to 1.8–2.4 V range. The output power of the boost converter is stored on a capacitor.

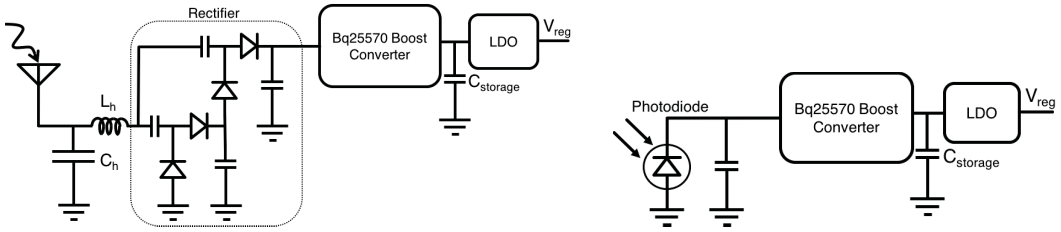

(a) RF Harvester (b) Photodiode based Harvester

Fig. 5. **Harvester Topologies.** The RF harvester uses a rectifier followed by a boost converter to convert RF signals to DC power. The solar harvester uses a boost converter to convert the low voltage output from a photodiode to DC power.

In harvesting systems, such as the battery-free phone, the power available from sources such as RF or ambient light can be lower than the active power consumption. To ensure that the phone can operate in these circumstances, we duty cycle the phone. The battery-free phone has two distinct modes of operation: sleep mode and active mode. In sleep mode, the cell-phone ceases all operations and enters the low power mode consuming minimal amount of power. In this mode, the phone is exclusively and efficiently harvesting energy. When the phone has harvested sufficient energy, it transitions into active mode to receive speech, transmit speech or communicate digital state with the basestation.

To implement duty cycling, the phone uses the voltage monitoring circuit of the bq25570 chip [2]. We set a lower and upper voltage threshold to 1.9 V and 2.4 V respectively on the storage capacitor. If the voltage on the storage capacitor drops below 1.9 V, the phone enters the sleep mode to minimize power and retain state. Once the voltage reaches the 2.4 V upper voltage threshold, it switches back to active mode of operation. The power harvester including the low-dropout regulator (LDO) consumes a total power of 2.2 μW.

4.1.1 RF powered phone. The RF powered phone uses a 2-stage Dickson charge pump rectifier topology to convert RF into DC power. We use SMS-7630 Schottky diodes from Skyworks [9] to efficiently harvest power in the 915 MHz ISM band. The rectifier is connected to the antenna via an LC matching network. The matching network ($L_h = 11\ nH, C_h = 6.2\ pF$) transforms the input impedance of the rectifier to match to the impedance of the antenna, which maximizes the RF signal at the input of the harvester. The low voltage DC output of the rectifier is fed to the boost converter (described in §4.1). We leverage the maximum power point tracking (MPPT) mode of the TI chip to tune the input impedance of the DC–DC converter to optimize impedance matching [37]. Specifically, we set the boost converter's MPPT reference voltage to 300 mV. Finally, the output of the boost converter is regulated by a low dropout (LDO) regulator to generate a stable supply rail, which is used to directly power different circuits on the cellphone. The RF energy harvester used in our implementation can work (cold start) down to a sensitivity of -13.4 dBm; this translates to a maximum operating distance of 32 feet.

In the RF powered phone, during the active mode of operation, the antenna is shared between the RF harvester and other components such as the backscatter microphone and AM receiver. Thus, the antenna is loaded by multiple elements, which results in reduction in the performance of RF energy harvesting and other functionalities. The power harvested by the phone in the active mode is reduced and the phone is forced to duty cycle by disconnecting all other blocks from the antenna and exclusively harvest power. In §4.2.1 we describe techniques which optimize the performance of the RF powered phone in active mode of operation.

4.1.2 Photodiode powered phone. We use VEMD5060X01 silicon PIN photodiodes by Vishay as our transducer to harvest power from ambient light [12]. Our minimum goal is to continuously operate the battery-free phone in ambient light settings of 500 Lux, found in typical homes and offices. We use fifteen photodiodes connected in parallel which generates at least 15 μW, the minimum power required for cold start of DC–DC converter when ambient light is greater than or equal to 500 Lux. Each VEMD5060X01 photodiode has an active area of 7.5 mm^2

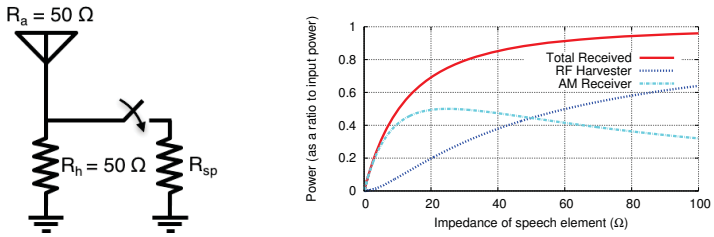

(a) Equivalent circuit for AM receiver (b) Power as a function of AM receiver's impedance

Fig. 6. **Optimizing speech reception on RF powered phone.** We analyze the equivalent circuit of an AM receiver to design an optimal matching network for speech reception on an RF powered phone.

and the combined photodiode used in our implementation has an effective area of 1.1 cm^2. This was sufficient for continuous operation of the battery-free phone in 500 Lux light settings.

We connect the photodiodes to bq25570 energy-harvesting chip. To maximize efficient of harvesting ambient light, we use the maximum power point tracking (MPPT) mode of the bq25570 chip and set the MPPT reference voltage to 80% of the open circuit voltage of the photodiode [2]. As before, the output of the boost converter is regulated by a low dropout (LDO) regulator to generate a stable supply rail.

4.2 Optimizing speech performance of the battery-free phone

We describe techniques to optimize transmission and reception of speech on the photodiode and RF powered battery-free phone.

4.2.1 RF powered phone. In the RF powered phone, a single antenna is used for energy harvesting, speech transmission as well as speech reception. Thus, the performance of RF energy harvesting or the amount of energy that can be harvested from incident RF signal is a function of the operating mode of the phone. Specifically, the phone spends most its time in the speech transmission and reception modes (compared to digital communication which lasts a few milliseconds). So, we focus to optimize these two modes.

Speech Transmission. To transmit speech, the RF powered phone connects the antenna to the backscatter microphone. However, the antenna is already connected to the RF harvester and it sees the backscatter microphone in parallel to the harvester. Thus, the input power is split between the harvester and the backscatter microphone. This impacts the performance of both the RF harvester and backscatter microphone. Since the backscatter microphone link from phone to basestation attenuates faster ($\propto \frac{1}{d^4}$), our goal is to optimize its performance.

Going back to the analysis conducted in §3.1, now the impedance seen by the antenna in an RF powered phone is a parallel combination of harvester (matched to antenna impedance) and the backscatter microphone. Using the same binomial approximation expression from before, the signal from an RF powered analog backscatter microphone can be written as,

$$S_{backscattered} \propto 1 + \Gamma = 1 + \frac{R_a - R_{\mu P}||R_a}{R_a + R_{\mu P}||R_a} = \frac{2R_a}{R_a + R_{\mu P}||R_a} \approx \frac{2}{R_a + 2R_0}\left[R_a + R_0 + \frac{V_{speech}}{V_p}\left(\frac{R_a R_0}{R_a + 2R_0}\right)\right] \quad (3)$$

To maximize the backscattered speech from the RF powered phone we set $R_0 = \frac{R_a}{2}$, i.e., we tune the impedance of the microphone ($L_{\mu P} = 15\ nH, C_{\mu P} = 0\ pF$) when there is no input speech to match half the impedance of the antenna. Due to the additional loading of the RF harvester, the performance of the RF powered backscatter microphone reduces by 3 dB when compared to photodiode powered backscatter microphone.

Speech Reception. To receive speech, the RF powered phone connects the antenna to the AM receiver. However, since the RF harvester always loads the antenna, the input power at the antenna is split between the energy harvester and the AM receiver. This impacts the performance of RF energy harvesting as well as the speech

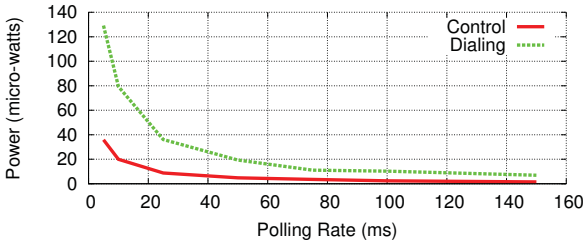

Fig. 7. **Power consumption of capacitive touch buttons.**

received by the phone. To understand how we optimize this system, consider the equivalent circuit diagram shown in 6(a) where R_h is the impedance of the RF harvester and R_{sp} is the impedance of the AM speech receiver. The total power received by the antenna as a fraction of the input power is a function of the impedance at the antenna and can be written as,

$$P_{total} = \left[1 - |\Gamma|^2\right] = \left[1 - \left|\frac{R_a - R_h||R_{sp}}{R_a + R_h||R_{sp}}\right|^2\right] \tag{4}$$

The power received by the harvester and the AM speech receiver can be represented as,

$$P_h = P_{total}\frac{R_h||R_{sp}}{R_h} \tag{5}$$

$$P_{sp} = P_{total}\frac{R_h||R_{sp}}{R_{sp}} \tag{6}$$

The total received power at the harvester and the AM receiver for a range of input impedances of AM receiver is shown in 6(b). The impedance of both the antenna and the harvester is 50 Ω (power matched for optimal harvesting). The plot show that as the impedance of the AM receiver is increased, the total received power increases. The AM receiver is in parallel with the 50 Ω harvester, so as the impedance of the AM receiver increases, the antenna sees an impedance closer to 50 Ω, which maximizes the total receiver power. However, the power received by the AM receiver is maximum (50% of input power) for 25 Ω but for this impedance of the AM receiver, the RF harvester only receives 20% of the input power. Since our cellphone is not limited by the performance of received speech (since the backscatter uplink attenuates faster), we tradeoff performance of speech reception for efficient RF energy harvesting. Specifically, we set impedance of the AM receiver to 50 Ω, which ensures that 88% of the input power is received and is split evenly (44% each) between the harvester and AM receiver.

The RF powered phone is simultaneously harvesting power and receiving speech from the amplitude-modulated signal. So, unlike the photodiode-powered phone, there exists a tradeoff between power harvesting and quality of received speech. The basestation can control the tradeoff by setting the value of the modulation index, m. A lower value of m is optimal for speech reception whereas a higher m increases available RF power. In §5 we study this tradeoff by setting m to 0.2, 0.5 and 1 and evaluating simultaneous RF energy harvesting and speech reception.

4.2.2 Photodiode powered phone. In the photodiode powered phone, the energy harvesting is decoupled from all other RF functionalities. Hence, the speech transmission and reception analysis and techniques described in §3 are directly applicable. Specifically, the matching network of the analog backscatter microphone is designed for $R_s = R_a$. Since, the photodiode powered phone does not harvest from RF, the basestation optimizes amplitude modulated for speech reception by setting $m = 1$. On the phone, we design the AM receiver matching network ($L_r = 7.5\ nH, C_r = 6.8\ pF$) to match the antenna of the phone which maximizes the power at the input of the AM receiver.

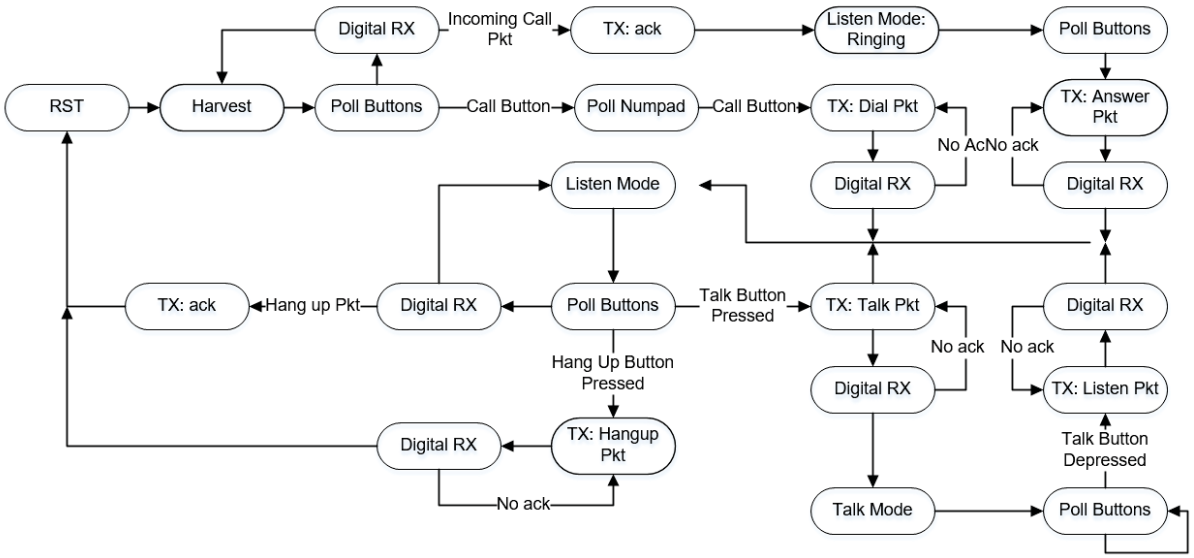

Fig. 8. **Battery-free cellphone state machine**

4.3 User Interface

The phone uses capacitive touch buttons and LED's for user interaction. The user dials the phone number and controls the phone using capacitive touch buttons. As shown in Fig. 2(b), the cellphone has twelve buttons for digits 0-9, * and # for dialing and two buttons *A* and *B* for control.

To respond to user input, we use the capacitive touch controller of the MSP430 micro-controller to continuously polls the capacitive touch inputs. However, since polling consumes power, there is a fundamental trade-off between power consumption and speed of interactivity. We evaluate the power consumption of capacitive touch buttons at different polling rates to determine optimal rate for our power budget.

We configured the cellphone to poll the buttons at different rates and used a Source Measuring Unit (SMU) to measure power. Fig. 7 shows the power consumption of the MSP430 (includes sleep mode current) for the two classes of buttons: control (poll only *A* and *B*) and dialing (poll all 14 buttons). As expected, polling less number of buttons results in lower current consumption. This is convenient because dialing only happens once at the very beginning of a call, while the control buttons are in use throughout the length of a call.

Additionally, we note that power is inversely proportional to polling rate and flatten out around 50 ms polling rate. This allows the battery-free phone to maintain a reasonable response time to user interaction while consuming micro-watts of power.

4.4 Digital state machine and interaction with the basestation

To send and receive phone calls, the battery-free cellphone interacts with the basestation to manage its operating state and connection status. Due to the extremely energy constrained nature of the system careful coordination between the basestation and the battery-free cellphone must be maintained to ensure a smooth and interactive call experience. This coordination is handled by state machines on the battery-free cellphone as shown in Fig. 8.

Call Setup: Initially, while not on a call, the battery-free cellphone waits in a low power mode. This allows the phone to harvest energy while waiting for the user to initiate a call or for the basestation to notify it of an incoming call. To detect if the user is initiating or responding to an incoming call, the phone periodically wakes from sleep mode to poll the "call" button and enter digital RX mode to listen for incoming data packets.

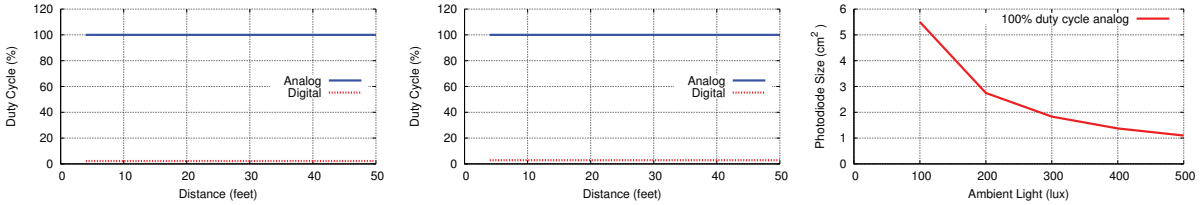

(a) Duty cycle while transmitting speech (b) Duty cycle while receiving speech (c) Photodiode size for 100% duty cycle

Fig. 9. **Photodiode Energy Harvesting.** The plots show the duty cycle of the battery-free phone for transmitting and receiving speech running on energy harvested from 500 Lux ambient light using photodiodes.We also show the minimum size of the photodiode for continuous operation as a function of ambient light conditions.

If the user presses the "call" button to initiate the call, the phone transitions to dialing state where it polls the buttons until the user presses the "call" button again. It then transmits a digital packet using backscatter to the basestation with the dialed phone number and enters digital RX mode to wait for an ACK. The basestation (always in an RX mode) receives the callpacket, parses the phone number, and sets up the call. Once the call is ringing, it transmits an ACK to the phone which transitions to "listen mode".

In the case of an incoming call, the basestation detects an incoming call, and transmits a digital downlink packet to the phone notifying it. The phone sends an ACK to the basestation and transitions to "listen mode".

Ongoing Call: While a call is in progress, the basestation manages transitions between speech transmission/reception, digital communication and ending the call. Immediately after dialing or connecting to an incoming call, the phone goes into speech "listen mode". By starting in the "listen mode", the user will be able to hear the ring on an incoming call or the answer of the other line. Due to the half-duplex nature of the system, the user cannot talk and listen at the same time. We use "push to talk" scheme: the phone defaults to listen mode and only transmits uplink audio while the "talk" button is being held. We note that this can result in the battery-free phone being able to talk over the other party on the call and interrupt them. However, given the asymmetric nature of the call between a regular phone and a battery-free phone, we believe this is a reasonable trade-off.

While in "listen mode", the basestation transmits speech using analog modulation and the phone periodically polls the control buttons and digital RX. Talking during a call is achieved using the aforementioned "push to talk". When the user pushes the "talk" button, the phone sends a digital packet to the basestation requesting a change of mode from listen to talk. After it receives and ACK, the phone turns on the microphone and backscatters speech. When it detects that the "talk" button has been released, it sends another packet to the basestation requesting to switch to "listen mode" and connects the speaker to the antenna when it receives the ACK.

Ending a Call: A call can be ended in two ways. The user can press the "hang up" button which the phone to send a digital packet to the basestation requesting to end to the call. After it receives the acknowledgment, the phone transitions back to the original low power state waiting for another call. Alternatively, if the other line hangs up first, the basestation processes the termination of the connection and transmits a hang up packet to the phone. The phone acknowledges the packet and enters the low power mode.

5 EVALUATION

In this section, we evaluate the performance of our battery-free phone in various operational modes. In particular, we start by evaluating the energy harvesting capabilities of the system while it is transmitting or receiving speech since these are the modes in which the phone operates for most time when in use. Next, we quantify the quality of speech that can be transmitted and received at the battery-free phone.

Basestation implementation. We implement our basestation with USRP X300 software defined radios with two UBX-40 RF daughter boards [10, 11]. The output power of the USRP is set to 30 dBm using the RF5110 RF Power amplifier [7]; this is within the maximum transmit power allowed by FCC in the ISM bands. We use a bi-static

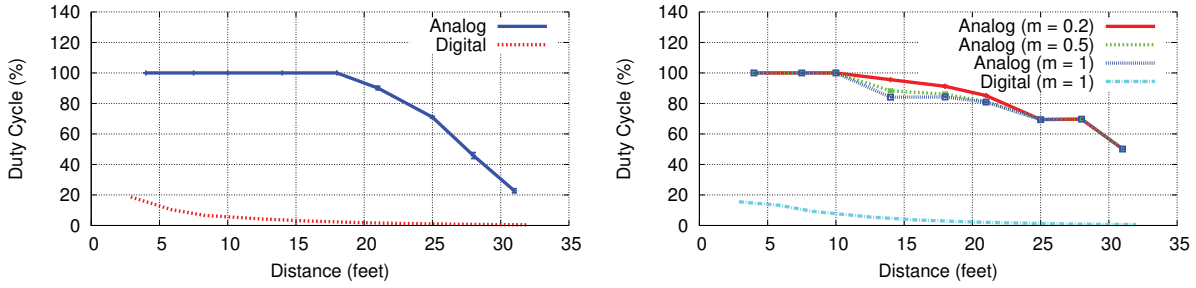

(a) Duty cycle while transmitting speech

(b) Duty cycle while receiving speech

Fig. 10. **RF Energy Harvesting.** The plots show the duty cycle of the battery-free phone for uplink and downlink communication while running on energy harvested from incident RF signals.

radar configuration for our backscatter basestation [28, 39]. The basestation transmits 915 MHz using the first daughter board into a 6 dBi circularly polarized antenna. Another 6 dBi antenna located 1.5 feet apart is used as the receive antenna and connects directly to the second UBX-40 daughter board configured as the receiver. The two identical patch antennas are placed at a height of 3 feet from the ground.

5.1 Energy Harvesting

We evaluate the harvesting capabilities of our battery-free phone using RF signals and photodiodes.

5.1.1 Photodiode Harvesting. One of the key benefits of harvesting energy using photodiodes, as described in §4.1.2, is that energy harvesting is decoupled from other RF communication functionalities of the phone. Thus, given the low operating power of our battery-free phone, a photodiode-harvesting phone can operate continuously or at very high duty cycles as long as there is enough ambient light. To evaluate this, we place our photodiode harvester in office environments and measure available power.

We configure the phone in speech transmission mode and place the prototype in an office space with ambient light intensity of around 500 Lux. We use an NI MyDAQ to monitor the operational state of the phone. We conduct a similar experiment when the phone is in speech reception mode. Fig. 9 plots the duty cycle, i.e., the percentage of the time the phone spends in active mode as a function of the distance between the basestation and the photodiode powered phone. For comparison, we also plot the duty cycle required by a digital design described in §1 that uses ADC, DAC and microcontroller to process speech. The plots show that when the phone uses analog backscatter to transmit speech and amplitude modulation to receive analog speech, the photodiode powered phone can operate continuously at 100% duty cycle under 500 Lux ambient light setting. However, in comparison a fully digital design has duty cycle rates lower than 2.5%. Since, the phone is harvesting power from ambient light, its duty cycle is independent of separation from the basestation. Finally, to illustrate how the photodiode phone can operate under different lighting conditions, Fig. 9(c) plots the size of the photodiode required to guarantee 100% duty cycle while using the analog approach for transmitting and receiving speech under 100-500 lux light conditions. We can see that even under the worst conditions of 100 lux, we only require a tiny 5.5 cm^2 active area photodiode.

5.1.2 RF Energy Harvesting. When the phone harvests power from incident RF signals, the antenna is simultaneously used for both RF energy harvesting and other functionalities such as speech reception and transmission. Thus, the performance of RF energy harvesting is a function of the operational mode of phone. We evaluate how the transmission and reception of speech impact the performance of RF energy harvesting.

RF Energy Harvesting while transmitting speech. We configure the battery-free phone to continuously transmit speech in active mode. Specifically, whenever the phone has sufficient energy on the storage capacitor, it connects the backscatter microphone to the antenna and transmits speech back to the basestation. We set the

basestation in one corner of the room and move the RF powered battery-free phone away from it in a straight line. We position the phone PCB prototype on a stand and orient the phone PIFA antenna parallel to the patch antennas of the basestation during our experiments. The basestation is setup to transmit a single tone signal, which is used for both analog audio backscatter and RF energy harvesting. We use an NI MyDAQ to monitor the operational state of the phone. At every distance between the basestation and the RF powered phone, we measure the percentage of the time the phone stays in the active mode, i.e., fraction of time it transmits speech compared to the sleep mode. Fig. 10(a) plots the duty cycle, i.e., the percentage of the time the phone spends in active mode as a function of the distance between the basestation and the RF powered phone. For comparison, we also plot the duty cycle required by a digital backscatter design that uses ADCs and a microcontroller to process the speech. The plots show the following:

- The phone operates at 100% duty cycle while it is transmitting speech up to 18 feet between the RF powered phone and the basestation. This means that the RF powered phone can continuously transmit speech with no interruption. This is because despite the loss due to the loading of the antenna by the backscatter microphone, the harvested power is still greater than the total power consumption of the phone and hence, the RF powered phone can continuously transmit speech with no interruptions.
- For distances greater than 18 feet and up to 31 feet between the phone and the basestation, fraction of time the phone can transmit speech to the basestation linearly decreases with distance. This is because less power is available at the antenna at larger distances. Specifically, beyond 18 feet, the harvested power when the antenna is loaded by the backscatter microphone is less than the total power consumption of the phone. Thus, whenever the voltage on the storage capacitor drops below the threshold, the phone disconnects the backscatter microphone from the antenna and goes into sleep mode to efficiently harvest RF power. Once sufficient energy is available on the storage capacitor, it transitions back to transmit speech. One approach is to choose the size of the storage capacitor to support a minimum time-period of continuous streaming and then wait for the phone to harvest power. Alternatively, for an additional 0.2 μW, instead of continuously streaming speech, the RF switch can be toggled at 8 kHz to transmit sampled analog speech which can be reconstructed by the basestation. By transmitting only sampled values, the fraction of the time the microphone is backscattering speech and antenna is loaded decreases. This relaxes the duty cycle requirement and also increases the available RF power. For example, 8 kHz sampling clock high for one-fifth of the time, reduces the time when the backscattered microphone is transmitting and available RF power by a factor of 5. So, even at the maximum operating distance of 31 feet, the microphone now transmits at 100% (20%*5) duty cycle. We note that in comparison, a fully digital design has duty cycle rates lower than 3% at distances greater than 18 feet.

RF energy harvesting while receiving speech. Next, we configure the RF powered phone to receive speech in the active mode where we connect our speech envelope detector circuit to the antenna. When the phone is in active mode, the basestation transmits speech using the amplitude modulation technique described in §3.2. However, when the phone transitions to sleep mode, the basestation transmits a single tone signal for the phone to efficiently harvest power. We study the performance of the system for three different amplitude modulation indexes: 0.2, 0.5 and 1. We again use an NI MyDAQ to monitor the operating state of the phone. We vary the distance between the basestation and the RF powered phone and measure the percentage of time the phone stays in active mode receiving speech. Fig. 10(b) plots the duty cycle, as a function of the distance between the basestation and the RF powered phone. The plots show the following:

- The phone operates at 100% duty cycle up to a distance of 10 feet. Specifically, the phone can continuously receive speech and actuate the earphones using only RF power. The operating distance for 100% duty cycle for receiving speech is less than transmission of speech because when the phone is receiving speech, the basestation is transmitting amplitude modulated signal which has lower power when compared to

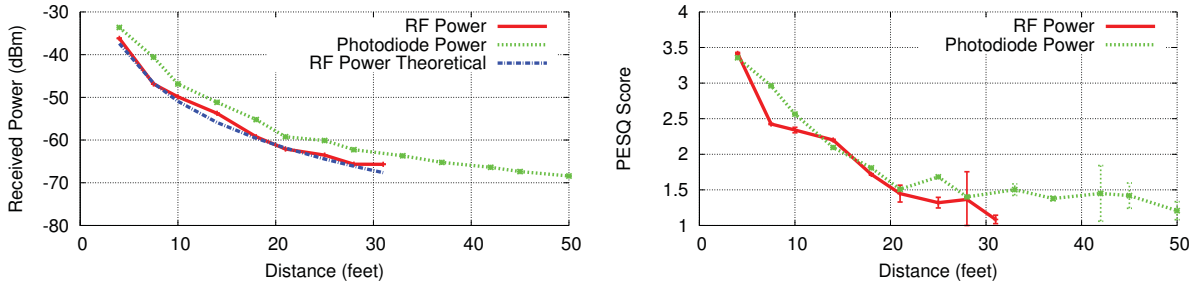

(a) Signal strength of backscattered tone received at the basestation (b) Quality of the backscattered speech received at the basestation

Fig. 11. **Speech transmission at the phone.** The plots show the signal strength of the backscattered tone and quality of the backscattered speech at the basestation.

a single tone signal which decreases the harvested power and consequently the operating range for 100% duty cycle operation. Note that this is not the case when we use photodiodes as our harvesting mechanism since it decouples harvesting and communication.

- For distances between 10 feet and 31 feet, the percentage of the time the phone can receive speech decreases as distance increases and modulation index decreases. A lower modulation index increases the average power of the RF signal that in turn increases the harvested power and the duty cycle of the RF powered phone. We also note that for similar distances, the duty cycle while receiving audio is higher than for transmitting audio. This is a result of the design of the matching network described in §4.2. The matching network for transmitting speech is optimized for speech performance whereas the matching network for receiving speech is optimized for RF power delivery.
- The battery-free phone can operate on RF power up to a distance of 31 feet with a duty cycle of 50% while receiving speech. This operating distance is same for speech transmission and reception mode because the maximum operating distance is determined by the sensitivity of the RF energy harvester. We also note that for comparison, a digital backscatter design has a duty cycle of 2.5% at a distance of 31 feet.

5.2 Speech transmission at the phone

Next, we evaluate the quality of the speech transmitted by the battery-free phone and received at the basestation. We configure the basestation to transmit a single tone signal at 915 MHz. The basestation uses the algorithm described in §3.1 to decode the speech from the backscattered RF signals. We use two metrics to evaluate the quality of the speech signal. First, we setup a speaker to transmit 1.75 kHz single tone signal at 80 decibels which is at a volume equivalent to a human directly speaking into a microphone. On the basestation, we measure the signal strength (in dBm) of this single tone speech signal as received by it. The signal strength is an indication of the SNR and the quality of the backscatter wireless channel between the basestation and the phone. Second, we setup the speaker to transmit a two second speech at the same 80 decibels to the microphone and measure the Perpetually Evaluation of Speech Quality (*PESQ*) metric of the received speech at the basestation. *PESQ* is a number between 0 and 5 and represents the quality of the speech signal, with 5 being the highest quality speech signal. A lower *PESQ* represents a lower quality speech signal. For all practical purposes such as human hearing and interpretation, a $PESQ \geq 1$ is considered to be sufficient [20]. We vary the distance between the battery-free phone and the basestation and plot the signal strength and the *PESQ* of the received signal in Fig. 11. We conduct experiments for both RF and photodiode powered phones. The plots show that:

- Fig. 11(a) shows that the signal strength of the received speech at the basestation decreases as the distance increases. This is expected because the backscattered signal experiences a path loss $\propto \frac{1}{d^4}$ where d is the distance between the battery-free phone and the basestation. At small distances, due to non-linearities in the JFET and the matching network, the received signal strength is slightly higher than the theory. The

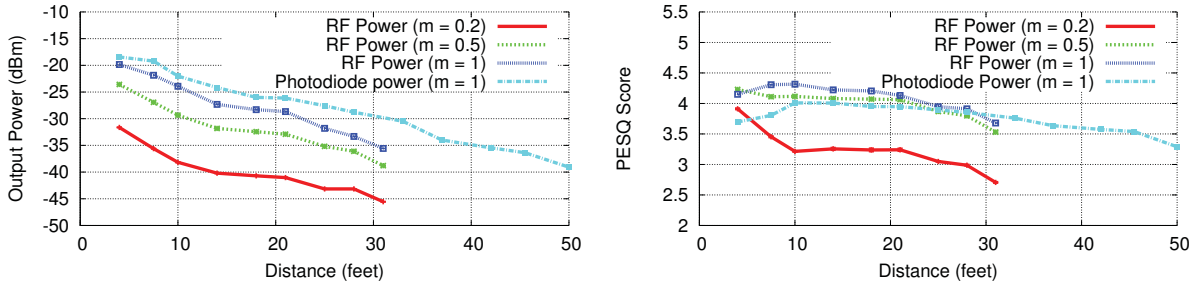

(a) Signal strength of tone received at the phone

(b) Quality of the speech received at the phone

Fig. 12. **Speech reception at the phone.** The plots show the signal strength and quality of speech received at the phone.

figure also shows that the signal strength of the received speech is 3 dB higher in case of a photodiode powered phone when compared to RF powered prototype. The photodiode powered RF front end is not loaded by the RF energy harvester and as a result the backscattered speech signal has a higher signal strength and this agrees with the theory and system design described in §3.1.

- The RF powered phone can operate up to 31 feet which is the maximum operating range of the RF energy harvester. However, when powered using photodiodes, the battery-free phone can operate at distances beyond 50 feet which was the length of the room in which we conducted our experiments.
- Fig. 11(b) plots the *PESQ* of the received speech as a function of the distance between the battery-free phone and basestation. As the distance increases, the signal strength of the received speech decreases which reduces the quality of the received speech and hence the *PESQ* reduces, reflecting the degradation in the quality of the speech signal. The figure also shows that the quality of speech received by the photodiode powered phone is slightly higher than that of RF powered phone. The *PESQ* of the speech received at the basestation is always greater than 1 for all evaluated operating distances. Hence the RF powered phone can transmit satisfactory speech up to 31 feet whereas the solar powered phone can transmit speech at least up to 50 feet from the basestation.

5.3 Speech Reception at the phone

Finally, we evaluate the quality of the speech signal received at the battery-free phone using the same metrics above. We configure the basestation in the speech transmit mode and the battery-free phone to receive speech. The basestation transmits two sets of speech signals, a single tone at 1.75 kHz and a 2 second speech using amplitude modulation at 915 MHz. We conduct experiments for three different amplitude modulation indexes: 0.2, 0.5 and 1. We use an NI MyDAQ to record the speech signal received by the earphones on the battery-free phone. We vary the distance between the battery-free phone and the basestation and plot the signal strength and the *PESQ* of the received signal in Fig. 12 for different modulation indexes. The signal strength is an indicator of the volume of the speech received by the headphones and indicates whether the passive driver circuit can generate sufficient power to actuate the earphones for human hearing. We conduct experiments for both RF powered and photodiode-powered phone. The plots show the following:

- Fig. 12(a) shows that the signal strength of the received speech at the battery-free phone decreases as the distance increases. This is because the backscattered signal experiences a path loss $\propto \frac{1}{d^2}$ where d is the distance between the battery-free phone and the basestation. The plots also show that the signal strength decreases with the modulation index. A lower modulation index results in smaller amplitude variations and lower power at the output of the passive driver for the headphones.
- The photodiode powered phone has a higher signal strength compared to the RF powered version at similar operating distances. This is because the RF front end of the photodiode powered version is not

loaded with the RF energy harvester and hence generates higher output power. We note that the RF powered phone can operate up to 31 feet — this is the maximum operating range of the RF energy harvester. The photodiode powered phone, on the other hand, can receive speech at operating distances beyond 50 feet which was the length of the room in which we conducted our experiments. Finally, -45 dBm was the minimum power of the speech received by the battery-free cellphone. We tested this signal level with five young healthy human subjects to verify that this power was sufficient to actuate the earphone at volume required for human hearing.

- Fig. 12(b) shows that the *PESQ* of the received speech at the phone also decreases for most part as the distance between the battery-free phone and the basestation increases. However, for very small operating distances and modulation index of 1, when the input power is high, there is a small drop in the quality of the speech. This can be explained by the fact that the passive envelope detector distorts the signal at higher power levels which slightly degrades the quality of the received signal.
- As before, the quality of speech received by the photodiode-powered phone is higher than that of RF powered phone. We also note that the *PESQ* of the received speech is significantly greater than 1 for all operating distances. Hence, the battery-free phone can receive speech up to 31 feet when RF powered and at least 50 feet when powered using photodiodes.

Audio clips of the backscattered speech and speech received at the battery-free phone for different operating distances and PESQs can be found at the following link:

https://youtu.be/ct_9JgpZWGA

5.4 Battery-free phone and Skype Interaction

We leverage VoIP capabilities to call phones in regular phone networks. Specifically, we use a Skype API to programmatically manage connection states at the basestation and transmit audio transparently to the battery-free phone. The Skype4Py project exposes an API to issue commands to control a Skype client. We use it to receive incoming calls, dial out, and place users on hold during power failures. However, because we are controlling a native Skype client, there is no API for reading or writing audio buffers to/from our basestation software. To work around this issue, we create a virtual audio device in Linux that allows us to set the default speaker for Skype and pipe this virtual audio device to a GNURadio audio source. In a similar way, we also create a virtual microphone to pipe audio form a GNURadio sink to the Skype client. Using these techniques, we can configure a custom basestation to act as a bridge between our battery-free cellphone and the legacy phone network, allowing the user to call anyone in the world using our battery-free phone.

6 RELATED WORK

Our work uses power harvesting and backscatter communication to enable a battery-free cellphone. In this section, we will discuss related work in these areas.

Power Harvesting. Solar, piezoelectric and thermoelectric harvesting has also been investigated for developing battery-free systems. However, solar based systems that can recharge phone batteries [8] require additional and often bulky and expensive solar cells [33]. Additionally, piezoelectric and thermoelectric devices can only operate in scenarios where sufficient vibrations and thermal gradient are available which limits their usability [29].

Early work on far field RF power delivery has shown that small amount of power ($1 - 100\mu$W) can be harvested from RFID signals to operate accelerometers [35], temperature sensors [35, 43], and cameras [27]. However, due to limitations of existing digital architectures, all aforementioned RF powered systems heavily duty cycling their operation. Recently, researchers have also shown that similar amounts of power can also be harvested from ambient TV signals [26, 34, 42], cellular transmission from base stations [32, 36, 41] and Wi-Fi [37, 38]. Our harvesting approach in the 915 MHz band is complementary to these approaches and we can combine multiple

ISM band including 915 MHz, 2.4 GHz and 5 GHz to harvest more power [30]. However, the available power is still insufficient to continuously operate existing digital systems necessitating our analog designs. Finally, our work is also related to recent efforts in simultaneous wireless information and power transfer (SWIPT) which tradeoff power delivery and information transfer [25]. Instead in this work, we simultaneously harvest power and transmit/receive analog speech and optimize the tradeoff between the two modes using impedance matching to enable continuous battery-free cellphone operation.

Backscatter communication. Our work is related to recent progress on backscatter communication using RFID [16, 19, 44], TV [26, 31], Wi-Fi [21, 22, 24], ZigBee [21], Bluetooth [15, 47] and FM [13] signals.

The closest to our work is work on computational RFID systems such as Blink [45] and Dewdrop [14]. These systems use harvested power in an efficient manner to optimize duty cycling and are orthogonal to our approach. Ekhonet [46] is a digital sensing system that optimizes the computational module in traditional digital systems to send sensor data at an order of magnitude lower power. However, the overall power consumption of the system *including clock, ADC and sensor* is two orders of magnitude higher power than our battery-free cellphone. The battery-free cellphone design is based on our earlier work on analog backscatter where we demonstrated an RF powered microphone operating at up to 10 feet from a reader [39]. This paper makes significant improvements to our earlier analog backscatter microphone design to extend the operating range to 50 feet. Additionally, we present optimizations and integrate an audio receiver and photodiode based harvesting to design a battery-free phone which can enable two-way communication with cellular networks up to 50 feet from a basestation.

7 DISCUSSION AND CONCLUSION

This paper presents the first battery-free cellphone design that consumes only a few micro-watts of power. In this section, we outline various avenues for future research to improve our design performance.

Operating Range. The current implementation of battery-free phone operates up to 50 feet with photodiode power. The operating range of our phone is determined by the performance of the analog backscatter microphone, which can be improved by using multiples techniques: First, our basestation currently transmits 30 dBm output power in the 915 MHz ISM band; the maximum power allowed by the FCC in the unlicensed bands. However, in licensed cellular bands, the basestation can transmit orders of magnitude higher power which will significantly increase the operating range of the analog backscatter microphone. Second, our current prototype repurposes an existing electret microphone (designed for voltage output) for analog backscatter. This creates only one-tenth of the maximum possible differential radar cross-section, which results in a weak analog backscattered speech signal. We believe that a microphone designed to maximize the differential radar cross-section will also increase the performance and operating range of analog backscatter microphone. Third, our USRP based basestation suffers from self-interference that limits backscatter performance. One can leverage recent progress on full-duplex radios or physically separate transmitter and receiver to improve the quality of the analog backscattered speech.

Networking multiple devices. Traditional networks use a combination of time division multiplexing (TDM) and frequency division multiplexing (FDM) to share the wireless spectrum across large number of devices. Our battery-free system can be scaled along similar lines. The basestation can co-ordinate communication with different devices by assigning time slot and frequency channel to each device. Multiple backscatter devices can then simultaneously transmit data and analog speech by using different (assigned) frequency offset to backscatter data and receive speech in different time slots. Exploring this however is not in the scope of this paper.

Security. The basestation and battery free phone can use existing security and encryption techniques to exchange digital state information and security keys. To secure speech communication between the battery-free phone and the basestation, one can leverage low power analog techniques. Analog speech in our system has a maximum SNR of 50 dB, which corresponds to 8 bits of resolution. The phone can use backscatter modulation (using additional

FET in parallel to the microphone) to add an 8-bit resolution pseudo-random analog signal to the backscatter speech. The basestation can subtract this pseudo-random signal from the received signal to retrieve the original speech. Similarly, on the downlink channel, the reader can also add an 8-bit random number to speech. The phone can then toggle the RF switch to subtract the 8-bit random number and retrieve the transmitted speech. The 8-bit pseudo-random signal can be either pre-coded into the phone (such as the SIM ID) or can be negotiated using the encrypted digital backscatter communication.

Additional functionalities & features. Our current battery-free phone design implements the basic functionalities of a phone (speech and data transmission and user input via capacitive touch). We believe that one can easily integrate additional functionalities into our battery-free design. E-ink displays operating on harvested RF and solar power have been demonstrated which can be used to add a display to the battery-free cellphone [17]. Additionally, in our prior work on AllSee [23], we have shown that user can interact using simple hand gestures while consuming only few micro-watts of power that can be harvest from RF and ambient light. We could integrate such low-power gesture recognition with our battery-free cellphone design.

8 ACKNOWLEDGMENTS

We thank the reviewers for helpful feedback on the paper. We would also like to thank Meiling Wu and Sam Crow for their help in software development and system implementation. This work was funded in part by awards from the National Science Foundation (CNS–1452494, CNS–1407583, CNS–1305072) and Google Faculty Research Awards. All four authors are co-founders of Jeeva Wireless Inc and hold equity stakes in the company.

REFERENCES

[1] ADMP801 by Analog Devices. http://www.analog.com/media/en/technical-documentation/obsolete-data-sheets/ADMP801.pdf.
[2] bq25570 by Texas Instruments. http://www.ti.com/lit/ds/symlink/bq25570.pdf.
[3] Cavity resonator microphone (also known as the Great Seal Bug). http://www.spybusters.com/Great_Seal_Bug.html.
[4] EK23024-00 Electret Microphone by Knowles. http://www.knowles.com/download/file?p=EK-23024-000.pdf.
[5] Moshi's Mythro. https://www.moshi.com/audio-earbuds-mythro-mic\.
[6] MSP430FR5969 Micro-controller by Texas Instruments. http://www.ti.com/lit/ds/symlink/msp430fr5969.pdf.
[7] RF5110 Power Amplifier by RFDM. https://www.digchip.com/datasheets/download_datasheet.php?id=1106230&part-number=RF5110
[8] Samsung Guru E1107. http://www.phonearena.com/news/Did-you-know-that-Samsung-launched-the-first-solar-powered-cell-phone_id67493.
[9] SMS7630-061 by Skyworks. http://www.skyworksinc.com/uploads/documents/SMS7630_061_201295G.pdf.
[10] UBX-40 RF daughterboards by Ettus Research. https://www.ettus.com/product/details/UBX40.
[11] USRP X300 by Ettus Research. https://www.ettus.com/product/details/X300-KIT.
[12] VEMD5060X01 by Vishay. http://www.vishay.com/docs/84278/vemd5060x01.pdf.
[13] Wang Anran, Vikram Iyer, Vamsi Talla, Joshua Smith, and Shyamnath Gollakota. 2017. FM Backscatter: Enabling Connected Cities and Smart Fabrics. In *Usenix NSDI*.
[14] Michael Buettner, Ben Greenstein, and David Wetherall. 2011. Dewdrop: an energy-aware runtime for computational RFID. In *Proc. USENIX NSDI*. 197–210.
[15] J.F. Ensworth and M.S. Reynolds. Every smart phone is a backscatter reader: Modulated backscatter compatibility with Bluetooth 4.0 Low Energy (BLE) devices. In *RFID, 2015 IEEE International Conference on*.
[16] Lingzhi Fu, Lirui Liu, Min Li, and Junyu Wang. 2012. Collision recovery receiver for EPC Gen2 RFID systems. In *Internet of Things (IOT), 2012 3rd International Conference on the*.
[17] Shyamnath Gollakota, Matthew S Reynolds, Joshua R Smith, and David J Wetherall. 2014. The emergence of RF-powered computing. *Computer* 47, 1 (2014), 32–39.
[18] RC Hansen. 1989. Relationships between antennas as scatterers and as radiators. *Proc. IEEE* 77, 5 (1989), 659–662.
[19] Pan Hu, Pengyu Zhang, and Deepak Ganesan. 2015. Laissez-Faire: Fully Asymmetric Backscatter Communication. In *Proceedings of the 2015 ACM Conference on Special Interest Group on Data Communication (SIGCOMM '15)*.
[20] Yi Hu and Philipos C Loizou. 2008. Evaluation of objective quality measures for speech enhancement. *IEEE Transactions on audio, speech, and language processing* 16, 1 (2008), 229–238.

[21] Vikram Iyer, Vamsi Talla, Bryce Kellogg, Shyamnath Gollakota, and Joshua Smith. 2016. Inter-technology backscatter: Towards internet connectivity for implanted devices. In *Proceedings of the 2016 conference on ACM SIGCOMM 2016 Conference*. ACM, 356–369.
[22] Bryce Kellogg, Aaron Parks, Shyamnath Gollakota, Joshua R. Smith, and David Wetherall. 2014. Wi-fi Backscatter: Internet Connectivity for RF-powered Devices. In *Proceedings of the 2014 ACM Conference on SIGCOMM*.
[23] Bryce Kellogg, Vamsi Talla, and Shyamnath Gollakota. 2014. Bringing gesture recognition to all devices. In *Usenix NSDI*.
[24] Bryce Kellogg, Vamsi Talla, Shyamnath Gollakota, and Joshua Smith. 2016. Passive Wi-Fi: Bringing Low Power to Wi-Fi Transmissions. In *Usenix NSDI*.
[25] Ioannis Krikidis, Stelios Timotheou, Symeon Nikolaou, Gan Zheng, Derrick Wing Kwan Ng, and Robert Schober. 2014. Simultaneous wireless information and power transfer in modern communication systems. *IEEE Communications Magazine* 52, 11 (2014), 104–110.
[26] Vincent Liu, Aaron Parks, Vamsi Talla, Shyamnath Gollakota, David Wetherall, and Joshua R Smith. 2013. Ambient backscatter: wireless communication out of thin air. *ACM SIGCOMM Computer Communication Review* 43, 4 (2013), 39–50.
[27] Saman Naderiparizi, Aaron Parks, Zerina Kapetanovic, Benajamin Ransford, and Joshua R Smith. WISPCam: A Battery-Free RFID Camera. In *IEEE RFID 2015*.
[28] Pavel V Nikitin and KV Seshagiri Rao. 2008. Antennas and propagation in UHF RFID systems. In *RFID, 2008 IEEE International Conference On*. IEEE, 277–288.
[29] Joseph A Paradiso and Thad Starner. 2005. Energy scavenging for mobile and wireless electronics. *IEEE Pervasive computing* 4, 1 (2005), 18–27.
[30] A.N. Parks and J.R. Smith. 2014. Sifting through the airwaves: Efficient and scalable multiband RF harvesting. In *IEEE RFID 2014*.
[31] Aaron N. Parks, Angli Liu, Shyamnath Gollakota, and Joshua R. Smith. 2014. Turbocharging Ambient Backscatter Communication. In *Proceedings of the 2014 ACM Conference on SIGCOMM*.
[32] Aaron N Parks, Alanson P Sample, Yi Zhao, and Joshua R Smith. A wireless sensing platform utilizing ambient RF energy. In *IEEE BioWireless 2013*.
[33] Vijay Raghunathan, Aman Kansal, Jason Hsu, Jonathan Friedman, and Mani Srivastava. 2005. Design considerations for solar energy harvesting wireless embedded systems. In *Proceedings of the 4th international symposium on Information processing in sensor networks*. IEEE Press, 64.
[34] Alanson Sample and Joshua R Smith. 2009. Experimental results with two wireless power transfer systems. In *Radio and Wireless Symposium, 2009. RWS'09. IEEE*. IEEE, 16–18.
[35] A.P. Sample, D.J. Yeager, P.S. Powledge, A.V. Mamishev, and J.R. Smith. 2008. Design of an RFID-Based Battery-Free Programmable Sensing Platform. *IEEE Transactions on Instrumentation and Measurement* 57, 11 (November 2008), 2608–2615.
[36] Hucheng Sun, Yong-xin Guo, Miao He, and Zheng Zhong. 2013. A dual-band rectenna using broadband yagi antenna array for ambient RF power harvesting. *IEEE Antennas and Wireless Propagation Letters* 12 (2013), 918–921.
[37] Vamsi Talla, Bryce Kellogg, Benjamin Ransford, Saman Naderiparizi, Shyamnath Gollakota, and Joshua R Smith. 2015. Powering the next billion devices with wi-fi. In *Conext*. ACM, 4.
[38] Vamsi Talla, Stefano Pellerano, Hongtao Xu, Ashoke Ravi, and Yorgos Palaskas. Wi-Fi RF energy harvesting for battery-free wearable radio platforms. In *IEEE RFID 2015*.
[39] Vamsi Talla and Joshua R Smith. 2013. Hybrid Analog-Digital backscatter: A new approach for Battery-Free sensing. In *RFID (RFID), 2013 IEEE International Conference on*. IEEE, 74–81.
[40] Desmond PC Thackeray. 1983. When tubes beat crystals: early radio detectors. *IEEE spectrum* 20, 3 (1983), 64–69.
[41] H.J. Visser, A.C.F. Reniers, and J.A.C. Theeuwes. Ambient RF Energy Scavenging: GSM and WLAN Power Density Measurements. In *EuMC 2008*.
[42] Rushi J Vyas, Benjamin B Cook, Yoshihiro Kawahara, and Manos M Tentzeris. 2013. E-WEHP: A batteryless embedded sensor-platform wirelessly powered from ambient digital-TV signals. *IEEE Transactions on microwave theory and techniques* 61, 6 (2013), 2491–2505.
[43] Jun Yin, Jun Yi, Man Kay Law, Yunxiao Ling, Man Chiu Lee, Kwok Ping Ng, Bo Gao, Howard C Luong, Amine Bermak, Mansun Chan, and others. 2010. A system-on-chip EPC Gen-2 passive UHF RFID tag with embedded temperature sensor. *IEEE Journal of Solid-State Circuits* 45, 11 (2010), 2404–2420.
[44] Pengyu Zhang and Deepak Ganesan. 2014. Enabling Bit-by-bit Backscatter Communication in Severe Energy Harvesting Environments. In *Proceedings of the 11th USENIX Conference on Networked Systems Design and Implementation (NSDI'14)*.
[45] Pengyu Zhang, Jeremy Gummeson, and Deepak Ganesan. 2012. Blink: A high throughput link layer for backscatter communication. In *Proceedings of the 10th international conference on Mobile systems, applications, and services*. ACM, 99–112.
[46] Pengyu Zhang, Pan Hu, Vijay Pasikanti, and Deepak Ganesan. 2014. Ekhonet: High speed ultra low-power backscatter for next generation sensors. In *Proceedings of the 20th annual international conference on Mobile computing and networking*. ACM, 557–568.
[47] Pengyu Zhang, Mohammad Rostami, Pan Hu, and Deepak Ganesan. 2016. Enabling Practical Backscatter Communication for On-body Sensors. In *Proceedings of the ACM SIGCOMM 2016 Conference on SIGCOMM*.

Received February 2017; revised April 2017; accepted June 2017